Waste biomass-based 3D graphene aerogel for high performance zinc-ion hybrid supercapacitors

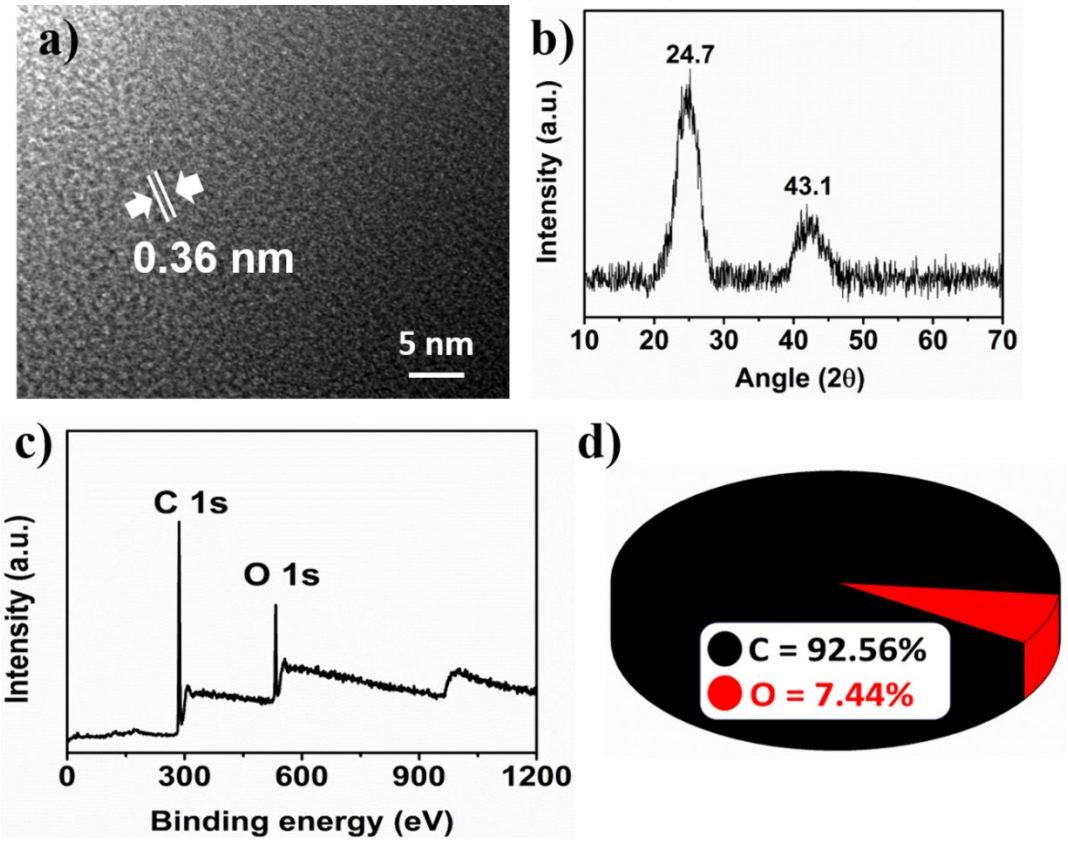

Fig. S1 Characterization of GAs. (a) HRTEM image. **(b)** XRD spectrum. **(c)** XPS spectrum **(d)** Elemental composition with percentage.

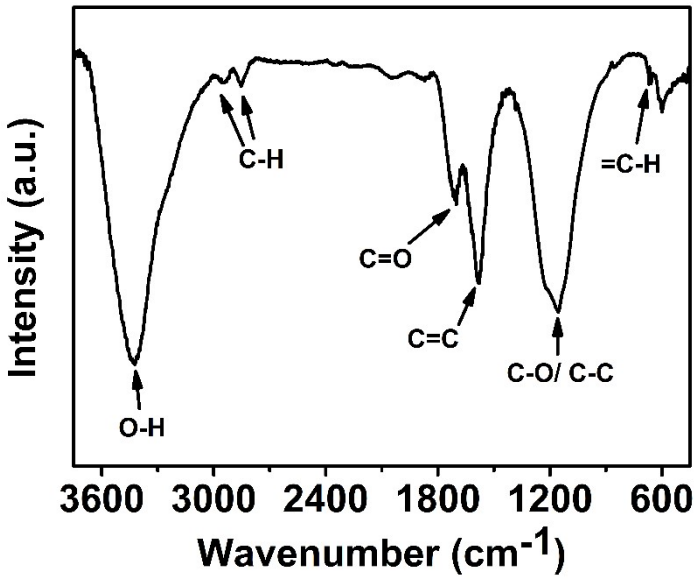

Fig. S2 FTIR spectrum of GAs.

Table S1: Comparison of the energy storage capabilities of ZHSCs utilizing GAs as cathode material with other reported carbon-based materials.

S. No.	Cathode material	Potential range (V)	Specific capacity	Energy density (W h kg^{-1})	Power density (kW kg^{-1})	Capacity retain after cycles	Ref.
1.	N/P co-doped graphene	0-1.8	210.2 F g^{-1}	94.6	4.5	almost100% - 15,000 cycles	[S1]
2.	graphene-based N/O co-doped porous carbon	0.2-1.8	117.8 mAh g^{-1}	88.9	0.10	87.2% - 10,000 cycles at 5 A g^{-1}	[S2]
3.	Graphene @ Zn	0.1-1.9	180 F g^{-1} at 1 A g^{-1}	78.32	8.01	-	[S3]
4.	Kelp-carbon	0-1.8	196.7 mAh g^{-1} at 0.1 A g^{-1}	111.5	6.9	95 % - 100 cycles	[S4]
5.	S, N -doped porous carbon nano-cube	0-1.8	331 F g^{-1} at 1 A g^{-1}	148.9	0.9	70 % - 10,000 cycles at 5 A	[S5]

						g^{-1}	
6.	Carbon nano onions	0-1.9	342 F g^{-1} at 0.5 A g^{-1}	164.33	8.2	83 % - 10,000 cycles at 10 A g^{-1}	[S6]
7.	Activated carbon	0-1.8	85.7 mAh g^{-1}	61.6	1.725	91% - 20,000 cycles	[S7]
8.	N, O co-doped porous carbon	0.2-1.8	138.5 mAh g^{-1}	110	20	~100% - 10000 cycles at 5 A g^{-1}	[S8]
9.	B/N co-doped porous carbon	0.2-1.8	127.7 mAh g^{-1} at 0.5 A g^{-1}	86.8	12.2	81.3%-6500 cycles at 5 A g^{-1}	[S9]
10.	Activated carbon	0.5-1.5	259.4 F g^{-1} at 0.05 A g^{-1}	29.9	-	~100% - 10000 cycles	[S10]
11.	Pear fruit derived GAs	0-1.8	353.1 F g^{-1} at 0.1 A g^{-1}	158.9	14.8	84.2%- 10000 cycles at 10 A g^{-1}	**This work**

Table S2: The comparison of Csp values obtained from CV and GCD curves

C_{sp} from CV curves		**C_{sp} from GCD curves**	
Scan rate	**C_{sp} (F g^{-1})**	Current density (A g^{-1})	**C_{sp} (F g^{-1})**
5 mV s^{-1}	320.8	0.1	353.1
10 mV s^{-1}	261.77	0.5	317
20 mV s^{-1}	207.1	1	285.8
40 mV s^{-1}	162.4	2	257.84
60 mV s^{-1}	134.8	4	220.4
80 mV s^{-1}	121.8	6	204.1
100 mV s^{-1}	114	8	194.64
		10	187.73

		20	171.7

Materials and Methods

Materials

Waste pears were collected from the local fruit market in Visakhapatnam, India. Polytetrafluoroethylene (PTFE), and conductive carbon (super -P) were procured from Sigma-Aldrich. Stainless steel (SS-304) mesh (200 micron) was purchased from online platform Amazon, India. Conductive carbon fiber fabric (50 microns porosity (%), electrical conductivity of 7 Ω cm^{-1}) was acquired from Fuel Cell Earth (Stoneham, USA). All chemicals were utilized in their original state without further treatment. All the experiments were performed through distilled water.

Synthesis of Graphene Aerogels

The ultra-light weight porous GAs was synthesized utilizing market rejected pear as a carbon precursor following the previously reported method.[S11] The peeled pear slices were washed with hot water and placed in a Teflon-coated autoclave reactor at 250 ℃ for 24 h for carbonization. The resulting hydrogel was washed to remove impurities. The residual water was removed followed by freeze-drying at -80 ℃ and 20 Pa pressure through the ice sublimation process. The as obtained aerogels were graphitized in an argon atmosphere at 1000 ℃ for 2 h into a tubular furnace at a 5 ℃ min^{-1} heating rate to obtain ultralight GAs. The as-synthesized graphene aerogel was collected after natural cool to room temperature.

Characterizations

The morphological and microstructural characterization of as-synthesized samples were evaluated from field-emission scanning electron microscopy (FE-SEM) (using JEOL JSM-7500F instrument, operating voltage 20 kV), as well as transmission electron microscopy (TEM) and high-resolution TEM (HR-TEM) (using FEI Tecnai G2 F30 instrument, operating voltage 200 kV). Powder X-ray diffraction (XRD) (Rigaku RINT-2000) was performed using Cu K_α radiation source for the identification of nature and phase of prepared sample. The TriStar 3000 instrument was utilized to determine the Brunauer-Emmett-Teller (BET) surface area, pore size distribution, average pore diameter and pore volume at liquid nitrogen

temperature using the BET nitrogen adsorption/desorption method. WITec Raman spectrometer was used to record the Raman spectrum of GAs at an excitation wavelength of 405 nm. X-ray photoelectron spectroscopy (XPS) was carried out for the confirmation of chemical composition and binding environment by using the ULVAC-PHI X electron system equipped with Al K_α as an X-ray source. FTIR spectrum was recorded (using Bruker Vector22 instrument) in the wavenumber range from 400 to 4000 cm^{-1} for the examination of functional groups of GAs.

Electrochemical measurements

The GAs based cathode was fabricated by mixing active material, PTFE and conductive carbon with a ratio of 8:1:1 (w/w). The slurry was coated and pressed onto stainless steel mesh. The anode was fabricated on fiber cloth of conductive carbon in the solution of zinc sulphate by electrodeposition method. Both the electrodes were dried under vacuum at 80 ℃ for 12 h and mass loading of the both electrodes were ~2 mg cm^{-2}. The electrochemical energy storage properties were evaluated by assembling a coin type (CR2032) cell. In detail, the cell was assembled through GA (cathode), Zn coated carbon fiber (anode), Whatman-42 filter paper (separator) and $ZnSO_4$ electrolyte (1.5 M). The AUTOLAB PGSTST-204 system was used to carry out the GCD, CV, and EIS electrochemical measurements.

The electrochemical calculation

The following equations have been utilized for the calculation of specific capacitance (C_{sp}), specific energy (E), and specific power (P) of GA based Zn-HSCs.

$$C_{sp} = \frac{I\Delta t}{V\, m} \qquad \textbf{(1)}$$

$$E = \frac{C_{sp}\, V^2}{2 \times 3.6} \qquad \textbf{(2)}$$

$$P = \frac{E \times 3600}{\Delta t} \qquad \textbf{(3)}$$

where Δt indicates discharge time, V represents working potential window, m is active mass and I is the current density during charging and discharging process of the device.

References

S1. Y. Zhao, H. Hao, T. Song, X. Wang, C. Li and W. Li, *J. Power Sources*, 2022, **521**, 230941.

S2. H. Liu, W. Chen, H. Peng, X. Huang, S. Li, L. Jiang, M. Zheng, M. Xu and J. Zhu, *Electrochim. Acta*, 2022, **434**, 141312.

S3. X. Zhang, C. Chen, S. Gao, X. Luo, Y. Mo, B. Cao and Y. Chen, *J. Energy Storage*, 2021, **42**, 103037.

S4. J. Zeng, L. Dong, L. Sun, W. Wang, Y. Zhou, L. Wei and X. Guo, *Nanomicro Lett.*, 2021, **13**, 1-14.

S5. H. Gupta, Y. Dahiya, H. K. Rathore, K. Awasthi, M. Kumar and D. Sarkar, *ACS Appl Mater Interfaces*, 2023, **15**, 42685-42696.

S6. G. S. Das, R. Panigrahi, S. Ghosh and K. M. Tripathi, *Mater. Today Sustain.*, 2024, **25**, 100656.

S7. H. Wang, M. Wang and Y. Tang, *Energy Storage Mater.*, 2018, **13**, 1-7.

S8. X. Deng, J. Li, Z. Shan, J. Sha, L. Ma and N. Zhao, *J. Mater. Chem. A.*, 2020, **8**, 11617-11625.

S9. Y. Lu, Z. Li, Z. Bai, H. Mi, C. Ji, H. Pang, C. Yu and J. Qiu, *Nano Energy*, 2019, **66**, 104132.

S10. P. Zhang, Y. Li, G. Wang, F. Wang, S. Yang, F. Zhu, X. Zhuang, O. G. Schmidt and X. Feng, *Adv Mater*, 2019, **31**, 1806005.

S11. G. S. Das, J. Y. Hwang, J.-H. Jang, K. M. Tripathi and T. Kim, *ACS Appl. Energy Mater.*, 2022, **5**, 6663-6670.